

Article

A Robust Fuzzy Equilibrium Optimization-Based ROI Selection and DWT-Based Multi-Watermarking Model for Medical Images

Surbhi Bhatia *  and Alhanof Almutairi * 

Department of Information Systems, College of Computer Science and Information Technology,
King Faisal University, Al-Ahsa 31982, Saudi Arabia

* Correspondence: sbhatia@kfu.edu.sa (S.B.); akalmutairi@kfu.edu.sa (A.A.)

Abstract: Image watermarking is the process of securely embedding a higher amount of information in the host object. These processes ensure authentication, image integration, and content verification. Several existing methods face complicated problems, such as security issues, robustness, and data leakage. Therefore, researchers developed specific methods for different applications. However, the performance of the currently obtained method was lower due to their low resistances. Therefore, to overcome this issue, we employed a novel technique, a fuzzy equilibrium optimization (FEO) approach, for embedding water image encryption. Initially, the raw image undergoes fuzzification to determine the critical point; thus, the intensity of the radial line selects a region of interest (ROI). Finally, the watermarking images are converted into a time-frequency domain via discrete wavelet transform (DWT), where the sub-band is converted based on value of magnitude. The proposed technique is analyzed using three medical image datasets, namely magnetic resonance imaging (MRI), ultrasound (US), and computed tomography (CT) datasets. However, all pixels in each sub-band are replaced to form a fully encrypted image, guaranteeing a watermarked reliable, secure, non-breakable format. Singular values are obtained for the encrypted watermarking image to provide high robustness to the watermarked image. After validation, the proposed fuzzy equilibrium optimization technique achieved higher robustness and security against different types of attacks. Moreover, the proposed FEO technique achieved a value of peak signal to noise ratio (PSNR) about 42.5 dB higher than other compared techniques.

Keywords: fuzzy equilibrium; discrete wavelet transform; water mark; sub-band; robustness; security



Citation: Bhatia, S.; Almutairi, A. A Robust Fuzzy Equilibrium Optimization-Based ROI Selection and DWT-Based Multi-Watermarking Model for Medical Images. *Sustainability* **2023**, *15*, 6189. <https://doi.org/10.3390/su15076189>

Academic Editor: Maxim
A. Dulebenets

Received: 14 February 2023

Revised: 21 March 2023

Accepted: 31 March 2023

Published: 4 April 2023



Copyright: © 2023 by the authors. Licensee MDPI, Basel, Switzerland. This article is an open access article distributed under the terms and conditions of the Creative Commons Attribution (CC BY) license (<https://creativecommons.org/licenses/by/4.0/>).

1. Introduction

In telemedical applications, the verification of authenticity and copyright for medical images play a major role. Telemedicine-based medical image diagnosis is carried out with different techniques such as X-ray, ultrasound scanning, etc. Verification in the medical field is an important application for ensuring the authenticity of patient data in the time of transition of medical image. Data hiding is used to conceal a piece of information secretly in the medical image such as the electronic patient report [1]. Recently, digital watermarking has become an important approach for protecting the legitimacy and copyright of medical images. The digital watermarking approach exhibits technologies and methods that embed data into the host such as digital data, audio, video, and image without modifying its quality [2]. Generally, digital watermarking techniques are used for authentication, broadcast monitoring, database indexing, and medical imaging. The watermarking methods use fragile, semi-fragile, blind, and robust watermarks to provide authentication and copyright protection. Watermarking schemes are classified into Region of interest (ROI) lossless watermarking scheme, zero watermarking scheme, and reversible watermarking scheme [3]. ROI is the important area where important diagnosis data is

presented in the medical images. In a reversible watermarking scheme, the authentication of a specific image is extracted from its watermarked image very accurately [4].

In digital images, watermarking secret data is embedded into the host image for ownership authentication. There are different watermarking schemes to insert the data into the host image. The easiest form of watermarking is the alteration of the least significant bit (LSB) of the host image, which is called a fragile watermark [5–7]. Generally, the technique is used for patient information and to identity verification. Moreover, the medical image watermarking algorithm can be categorized into the authentication and integrity control (AIC) algorithm, data-hiding algorithm, and a combination of data-hiding algorithm as well as AIC [8,9]. The AIC algorithm aims to ensure the integrity and identity of the source image [10]. There are different applications of digital watermarking, such as content and image authentication, fingerprinting, tamper-proofing, digital rights management, and copyright protection, etc. The better way of performing watermarking is by ensuring that the image quality is not degraded and not affected by any attacks. This proposed work improves the image quality, security and reliability through the medical image watermarking process.

The selection of the optimal parameters for the previous method can be time-consuming and computationally expensive, which may limit its practical application in certain contexts. The quality of the watermarked images can be affected by the amount of noise and distortion in the original images, which may limit the robustness of the watermarking process. The novelty of this work is the integration of fuzzy logic and equilibrium optimization with image watermarking. The use of fuzzy equilibrium optimization (FEO) for ROI selection and embedding watermark images into the medical images is a unique approach. This method ensures a high degree of robustness and security against different types of attacks on the watermarked images. Furthermore, the use of discrete wavelet transform (DWT) to convert the watermark images into the time-frequency domain and the selection of optimal DWT layers for each medical image dataset is also a novel contribution. This approach ensures a high level of accuracy in the watermarking process and improves the quality of the watermarked images.

Motivation and Contribution

The proposed technique for image watermarking in medical images can contribute to sustainability in several ways. Firstly, the proposed technique provides a reliable and secure method for watermarking medical images, which can be used to protect patient data and prevent unauthorized access to sensitive information. This can help to ensure the privacy and confidentiality of patients, which is an important aspect of sustainability in the healthcare industry. Secondly, the proposed technique employs a fuzzy equilibrium optimization (FEO) approach for embedding water image encryption, which enhances the robustness and security of the watermarking process. This can help to prevent data leakage and ensure the integrity of medical images, which is essential for accurate diagnosis and treatment. By enhancing the reliability and security of medical images, the proposed technique can contribute to sustainable healthcare practices. Finally, the proposed technique can also contribute to sustainability by reducing the need for repeated medical imaging procedures. By providing a secure and reliable method for watermarking medical images, the proposed technique can help to prevent the loss or corruption of images, which can lead to the need for repeated imaging procedures. This can help to reduce the use of resources and minimize the environmental impact of healthcare practices. The research fulfils the scope of sustainability in healthcare for social development very well. The major contributions of the current study are as follows:

- The fuzzy equilibrium optimization (FEO) algorithm is proposed to provide secure, reliable and unbreakable watermarking for medical images.
- The medical image dataset is selected, which includes magnetic resonance imaging (MRI) images, computed tomography (CT) images and ultrasound (US) images for analysing the image quality.

- For determining the performance rate, a few performance evaluation measures such as embedding rate, embedding time, extraction time, coefficient index and entropy index are utilized.

The remaining section of this paper is arranged as follows. Section 2 presents the literary works based on a watermarking algorithm for medical images. Section 3 analyzes the basic concept of fuzzy logic and equilibrium optimization. Section 4 describes the proposed methodology. Section 5 portrays the experimental results obtained in the investigation of the performance of the proposed approach. Finally, Section 6 concludes the paper with a future scope.

2. Literature Survey

To achieve content authentication and tamper localization in secured telemedicine, Swaraja, K et al. [11] developed a framework with blind dual medical image watermarking. This method was used to prevent the alteration of content. In the medical image, the region of non-interest (RONI) blocks were used to hide the dual watermarks for authentication and recognition. This framework demonstrated its superior capabilities and outperformed the other related optimized hybrid algorithms. This method retrieved the original region of interest (ROI) without any loss of information. Liu, X et al. [12] developed a reversible water marking technique to safeguard the integrity and authenticity of medical images. The region of interest (ROI) watermarking entailed the risk of spatial image segmenting. The ROI method had failed in the recovery of tampered areas. In this method, recursive dither modulation (RDM) is used to avoid diagnostic biases. Singular value decomposition and slantlet transform combined with RDM are used to protect image authenticity. This method outperformed all the other techniques for medical image protection.

Zeng, C et al. [13] proposed a multi-watermarking algorithm on KAZE DCT for medical images. The features of the medical images were extracted with KAZE DCT and the sequent features of medical images were obtained with perceptual hashing. The multi-watermark images were encrypted by chaotic mapping. This method resulted in effective extraction of watermarks. This method could witheld both geometric and common attacks. Patel, N et al. [14] developed a DCT DWT hybrid ROI image compression for the application of telemedicine. This method recreated the medical image rapidly and eliminated the unwanted medical data with a compression algorithm. This method increased the data processing speed. The highest PSNR and lowest MSE were obtained using this technique. The best visual image was presented with this DCT compression method. It had bit rates higher than those obtained using wavelet compression algorithms.

Hu, K et al. [15] developed the zero watermarking algorithm used in medical field. The developed zero watermarking algorithm generated bi-dimensional empirical mode decomposition (BEMD) to detect the tampering regions. The images were divided into a number of residues and intrinsic mode functions (IMF). The singular value decomposition was used to extract feature matrices from the first IMF. Arnold transform was used in encrypting the watermark image to add security. The exclusive or operation was used to create feature images. These feature images were used to detect tampering and authenticate copyright. This algorithm created natural images and performed better than other algorithms in fighting various cyber-attacks. Nazari, M and Mehrabian, M. [16] developed a blind watermarking technique with integer wavelet transform (IWT) and least significant bit (LSB) for secured transmission of medical images. In this method, chaotic sequences were used to determine the host blocks locations and to encrypt watermark. A robust security level was achieved with the chaotic sequences. The ROI and the RONI were two divided parts of the image. The ROI data was not embedded due to high sensitivity. This method achieved 75 dB of PSNR value and provided highest imperceptibility. The embedded watermark's size was increased.

Gong, C et al. [17] illustrated a zero-watermarking algorithm on chaotic map and Harris SURF DCT for medical images. The established algorithm was used to exhibit the corners of the image. The descriptor matrix was created through the description of

extracted corners in the SURF algorithm. The watermark was encrypted with the logistic map algorithm. The developed method obtained the water mark without any changes in the medical image. This algorithm performed better in defending geometric attacks. Dhall, S. and Gupta, S. [18] proposed a highly secured multilayer watermarking mechanism for the purpose of medical applications. The proposed method was used to secure the medical images and the transcript of patient. The original medical image was embedded with electronic patient records (EPR) to obtain the watermarked image. The quantum encrypted and compressed EPR was embedded into the lifting wavelet transform (LWT) medical image. The image stenography technique was used to change the structure of the watermarked medical image and it also avoids the images from attacks. Hash algorithm with biometric detection was used for authentication. This method presented a highly secured health care system. This method consumed more time than other conventional methods due to multilayer security.

While some studies have developed effective watermarking techniques using methods such as blind dual watermarking, reversible watermarking, and zero watermarking, none of these studies have explored the possibility of combining these techniques to improve overall performance. Additionally, the studies mentioned have primarily focused on protecting the integrity and authenticity of medical images; however, there may be a need to also consider the protection of patient privacy and sensitive information.

3. Basic Concepts

The basic concepts employed in this paper are discussed as follows:

3.1. Fuzzy Logic

The fuzzy is explained based on membership function instead of the attribute function. The value of the membership function is either null or one [19,20]. The probability of all objects in the element collection is referred to as the membership function. The value of membership functions lies within the range [0, 1]. When the object is present in the collection, the membership function value is zero. When there is no object in the collection, the value of the membership function is one. The fuzzy logic control utilized conditional expressions such as if-then conditions rather than formulas to describe the control method. The conditional derivation is also known as inference. The interference is used for every propositional truthfulness validation. The FL control is classified into three phases, namely fuzzification, condition valuation, defuzzification.

Fuzzification

The fuzzy logic control system is executed by fuzzy rules, which are as follows:

Condition 1: If S is represented as u_1 and T is represented as v_1 , then X is denoted as h_1 .

Condition 2: If S is signified as u_2 and T is signified as v_2 , then X is denoted as h_2 .

From the above conditions, the condition variables are represented as S and T . The fuzzy parameters are classified by three membership functions which are denoted as u_1 , v_1 , and h_1 , respectively. The response variable is represented as X . The Mamdani provided a fuzzy inference procedure for the two conditions because the fuzzy rules are calculated as one. The membership function intervals are denoted as Y_1 and Y_2 . The membership rules variables are denoted as condition1 for $\eta_{u1}(s)$ and condition 2 for $\eta_{v1}(s)$.

Condition valuation

The control rules in the rule base are satisfied as $S = s$ and $T = t$. The conditional variables are represented below.

Condition 1: $\eta_1 = \eta_{u1}(s) \wedge \eta_{v1}(t)$

Condition 2: $\eta_2 = \eta_{u2}(s) \wedge \eta_{v2}(t)$

From the above condition, η_1 is the minimum function of truth degree for condition 1. η_2 is the minimum function of truth degree for condition 2. The expression of Mamdani-type rule validation is \wedge . The interval of the output variable is represented as

Y₃. The membership function of every fuzzy logic control output is the addition of all the membership functions.

$$\eta_h(X) = \eta_{w1}(X) * \eta_{w2}(X) \quad (1)$$

From the above equation, the expression for the maximum function of Mamdani-type condition validation is denoted as *.

Defuzzification

The fuzzy logic control system's input function is received by transforming the inference result into real value. The non-fuzzy result is used to determine the desirable output. The quantitative output of the fuzzy logic control system is expressed from the function $v_{hm}(X)$. The area of gravity method (Coa) is improved by using the expression of defuzzification, and is formulated as follows:

$$A_{Coa} = \frac{\int_a v_F(A) A k a}{\int_a v_F(A) A k} \quad (2)$$

The above equation \int_a signifies the integral of the every element membership function in the output fuzzy subset in the continual domain A.

3.2. Equilibrium Optimizer (EO)

In this section, the mathematical model, inspiration and equilibrium optimizer (EO) algorithm are presented.

Inspiration

The thoroughly mixed vigorous mass balance in the volume helped to delineate the inactive constituent of several sink and source mechanisms functions [20]. After penetration, the generated function is summed up and excluded from the leaved amount in this system. The inspiration for the EO approach is expressed in the equation below.

$$W \frac{dB}{ds} = V_f B_{equilibrium} - V_f B + M_{Gen} \quad (3)$$

where V_f denotes the volumetric flow rate, $W \frac{dB}{ds}$ represents a rate of mass change in the control volume, M_{Gen} denotes mass generation rate, $B_{equilibrium}$ is the concentration at an equilibrium state and B indicates the mass generation rate. For solving the concentration, Equation (1) is arranged into

$$\frac{dB}{\delta B_{equilibrium} - \delta B + \frac{M_{Gen}}{W}} = ds \quad (4)$$

The integration of Equation (2) is expressed in Equation (3).

$$\int_{B_0}^B \frac{dB}{\delta B_{equilibrium} - \delta B + \frac{M_{Gen}}{W}} = \int_{s_0}^s ds \quad (5)$$

$$B = B_{equilibrium} + (B_0 - B_{equilibrium})G + \frac{M_{gen}}{\delta W}(1 - G) \quad (6)$$

where

$$G = \exp[-\delta(s - s_0)] \quad (7)$$

From the above equations, δ represents the turnover rate, s_0 initial time concentration and B_0 indicates the initial start time. In the PSO algorithm, the particle related to the concentration and solution is analogous to the position of the particle in the PSO algorithm. Every term and way that impacts the search pattern is defined as follows.

Evaluation of initialization and function

The usage of the initial population by the EO algorithm helps in initializing the optimization process. In the search space, the initial concentration of the function is based on the dimensions and the particles.

$$B_j^{ini} = B_{\text{minimum}} + \text{random}_j(B_{\text{maximum}} - B_{\text{minimum}}) \quad j = 1, 2, 3, \dots, m \quad (8)$$

From the above equation, random_j indicates j th particles' initial concentration vector, B_j^{ini} indicates the initial concentration vector, m is the number of the particles, B_{minimum} represents the minimum values for the dimensions and B_{maximum} indicates the maximum values for dimension.

Equilibrium pool and candidates ($B_{\text{equilibrium}}$)

The last convergence state is the equilibrium state that tries to achieve the global optimum. The determination of the equilibrium state has taken place in the beginning without the knowledge of the equilibrium state in enabling the search pattern in favor of particles. Alpha, beta and gamma are, to date, the best candidates utilized by the grey wolf optimizer (GWO) in updating the other wolves' positions. This method's performance in the multimodal and composition function is degraded with the enhancement of unimodal functioned results by using less than four candidates. When the candidates' rate is more than four, the effect would be the opposite. The mathematical expression of the equilibrium pool and candidates are expressed in the form of numeric.

$$\vec{B}_{\text{equilibrium.pool}} = \left\{ \vec{B}_{\text{equilibrium}(1)}, \vec{B}_{\text{equilibrium}(2)}, \vec{B}_{\text{equilibrium}(3)}, \vec{B}_{\text{equilibrium}(4)}, \vec{B}_{\text{equilibrium(average)}} \right\} \quad (9)$$

In every iteration, every particle is updated the concentration by the selection among the candidates with the same probability. Based on this $\vec{B}_{\text{equilibrium}(1)}$, all the concentrations are updated by the first particle in the first iteration. $\vec{B}_{\text{equilibrium(average)}}$ -based concentrations are updated in the second iteration. Every particle is experiencing the process of updating with the whole candidate solutions and acquires the approximate number of updates till the end of the optimization process.

Generation rate (GR)

In the proposed EO algorithm, the generation rate enables an accurate solution with the enhancement of the exploitation phase. The multipurpose model explains the generation rate, which is expressed mathematically in the equation below.

$$\vec{GR} = \vec{GR}_0 e^{\vec{l}(s-s_0)} \quad (10)$$

$$\vec{GR} = \vec{GR}_0 e^{-\delta(s-s_0)} = \vec{GR}_0 \vec{G} \quad (11)$$

where

$$M_0 = \vec{G}_{cp} \left(\overrightarrow{B_{\text{equilibrium}}} - \vec{\delta B} \right) \quad (12)$$

$$\vec{G}_{cp} = \begin{cases} 0.5q_1 & q_2 \geq GP \\ 0 & q_2 < GP \end{cases} \quad (13)$$

In the above equation, \vec{G}_{cp} represents the generation rate control parameter, q_1 and q_2 represents the random numbers. The EOs updating rule is expressed in the equation below.

$$\vec{B} = \vec{B}_{\text{equilibrium}} + (\vec{B} - \vec{B}_{\text{equilibrium}}) \cdot \vec{G} + \frac{\vec{GR}}{\vec{\delta W}} (1 - \vec{G}) \quad (14)$$

where

$$G = b_1 \text{sign}(\bar{s} - 0.5) \left[e^{-\vec{\delta}s} - 1 \right] \quad (15)$$

From the above equation, W denotes the unit and G indicates the exponential term.

Memory Saving (MS) of the particle

The procedure of memory saving guides every particle to track the coordinates continuously in the space, and the fitness value is informed. This mechanism is helpful for the exploitation ability but caught in local minima when the global exploration ability has not benefitted this method.

Exploration capability of EO

In EO, various mechanisms and parameters result in exploration for the summarization of these terms.

- i. B_1 rules the algorithm's exploration ability and determines the potentiality of the equilibrium candidate's new position. As the value of B_1 increases, the exploration capability also increases. Moreover, the performance of the exploration is degraded by a number greater than three. B_1 is large enough in expanding the exploration ability because of its ability in magnifying the concentration variable. The sum of the cognitive and social parameters must be less than or equal to four in PSO.
- ii. $\text{Sign}(q - 0.5)$: The direction of exploration is controlled by sign. There is an equal possibility of positive and negative signs because of q in the range of $[0, 1]$ along with uniform distribution.
- iii. *Generation Probability* ($GP = 1$): The generation rate updated the concentration's participation probability, which is already controlled by GP. In the process of optimization, no participation of the generation rate term is represented as $GP = 1$. This condition reveals the greater ability of exploration and results in inaccurate solutions. Moreover, the participation of the generation rate term in the optimization process is denoted as $GP = 1$. It maximizes the stagnation probability in local optima. A good balance between exploitation and exploration is offered by $GP = 0.5$, on the basis of empirical testing.
- iv. *Equilibrium Pool*: The five particle is contained in this vector and the choosing of these particles is based on empirical testing. The distance between the candidates is very far from each other in the initial iterations. On the basis of these candidates, the concentrations are updated and enhance the ability of the algorithm in order to discover the space. In the initial iterations, the unknown search is discovered with the help of the average particle, as the particles are distant from each other.

Exploitation capability of EO

The local search and exploitation performance is carried out by using the important parameters and mechanisms.

- a. B_2 is the same as B_1 that rules the exploitation feature and determines the exploitation's magnitude by obtaining the best solution around.
- b. The $r - 0.5$ rules regarding the quality of exploitation and the local search direction are specified.
- c. *Memory saving*: The best particles which very far are saved by the memory saving and replaced by the worse particles. Moreover, these features enhance the ability of EO for exploitation.
- d. *Equilibrium pool*: The fade in of exploitation and fade out of exploration happens in the iteration lapse. Finally, the equilibrium candidates are very near each other in the final iteration and the concentration updating process helps the candidates around in the local search, resulting in exploitation.

4. Proposed Methodology

The proposed approach is initiated by determining the ROI with source medical image by using fuzzy equilibrium optimization (FEO) and DWT. The medical image watermarking

approach is presented by FEO-based ROI selection and the DWT method for embedding the encrypted watermark. In fuzzification, the critical points are evaluated by utilizing central and final intensity with a radial line to select the ROI. The watermark images are converted into a time-frequency domain by using DWT. According to the magnitude value, the sub-bands are interchanged through DWT. In the sub-bands, the pixels are swapped then the results showed that the watermark is assured to unbreakable form, reliable, and secure in the fully connected image. Figure 1 illustrates the proposed medical image watermarking process.

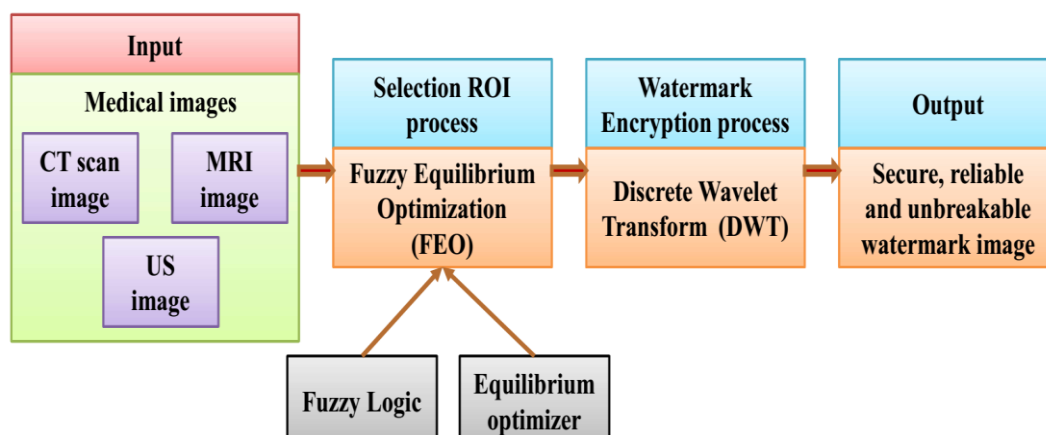


Figure 1. Proposed medical image watermarking process.

4.1. Fuzzy Equilibrium-Based Region of Interest (ROI) Selection

As regards the embedment of the watermark, using ROI regions recreates the pixels and leads to the wrong diagnosis [21]. In contrast, embed watermarks are used by the region of non-interest (RONI) watermarking in insignificant regions of medical diagnosis. However, the existing RONI is only able to execute and attach the information based on size but may not be safeguarded against a nasty attack. In this research, the medical image watermarking method uses a wavelet transformation approach and fuzzy-based region of interest (ROI) selection for the embedment of the encrypted watermark. Figure 2 depicts the flowchart of fuzzy equilibrium.

Fuzzy equilibrium

The fuzzy system is developed for the enhancement of memory rate efficiency. Here, the memory rate and generation rate are the input variables [22]. For output variables, the bar controller is used in adjusting memory saving (MS) and generation rate (GR). The movement of bar middle bar to the left minimizes the generation rate (GR). However, the movement toward the right minimizes the memory-saving (MS) phase. The memory rate is emphasized by fuzzy equilibrium. The fuzzy equilibrium are categorized into three types are as follows.

Fuzzification

The productivity of the students is measured by computing the generation rate (GR) and Memory rate. Moreover, from the five triangular membership functions with three triangles, right triangles and left triangles are used for the output variable.

Inferencing process

The conditional statements comprised of fuzzy logic are formulated by the Mamdani-type rule. The existing inputs are mapped with the fuzzy inference of Mamdani. The recommended fuzzy rules are as follows:

Rules:

- I. The movement of the bar is neutral when the success rate of the memory rate and generation rate is low.
- II. The movement of the bar is left, when the success rate of the generation rate and memory rate is low and medium.

- III. The bar movement is far-left if the success rate of the generation rate and memory rate is low and high.
- IV. The bar movement is right, as the generation rate and memory rate are medium and low.
- V. The movement of the bar is neutral when the generation rate and memory rate are medium.
- VI. The movement of the bar is left, when the generation rate and memory rate are medium and high.
- VII. The bar movement is right, as the generation rate and memory rate are high and low.
- VIII. The bar movement is right, as the generation rate and memory rate are high and medium.
- IX. If the success rate of memory rate and generation rate is high, then the movement of the bar is neutral.

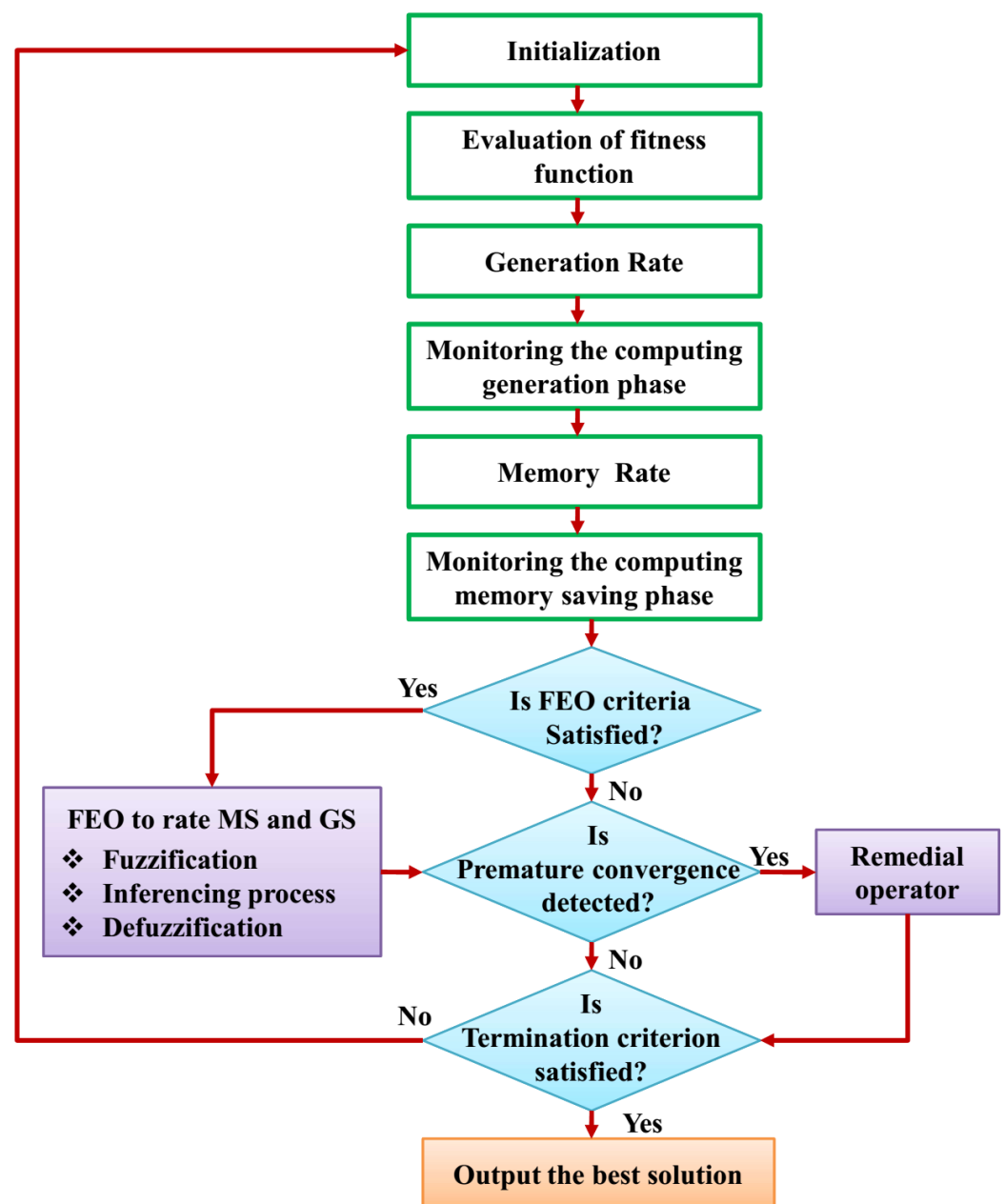


Figure 2. Fuzzy equilibrium flowchart.

Defuzzification

The defuzzification step is the opposite step of fuzzification. After completing the interference phase, the defuzzification starts. This process selects the center-of-sums method. The bar movement is the result of the fuzzy technique.

Remedial operator

In the remedial operator phase, a pre-mature convergence is considered when there is no fitness development over a long period or when the whole populations converge on a single solution.

4.2. Discrete Wavelet Transform (DWT) Based Watermark Encryption Process

The pre-processing watermark generates the bitstream for the embedding process [23]. A new optimal watermarking method is developed for embedding the higher capacity data by using DWT. In this section, the DWT optimizes the problems by the enhancement of existing solutions. The wavelet is converted into a water image for providing the fully encrypted image by using DWT.

Let us assume $y(\tau)$ is the integral factor, which is expanded based on wavelet bias function commonly referred to as continuous wavelet transform of $y(\tau)$. The expression to determine the wavelet bias function is formulated as follows:

$$\vartheta_{b,c}(\tau) = \frac{1}{\sqrt{|b|}} \Gamma\left(\frac{\tau - c}{b}\right), b \neq 0, c \in \mathbb{R} \quad (16)$$

The continuous wavelet transform is computed and expressed as follows:

$$\vartheta_y(b, c) = \langle y(\tau), \vartheta_{b,c}(\tau) \rangle = \frac{1}{\sqrt{|b|}} \int_{\mathbb{R}} y_{\tau}(\tau) \overline{\Gamma\left(\frac{\tau - c}{b}\right)} d\tau \quad (17)$$

From the above equation, the scale parameter is represented by b , time center parameter is indicated by c . If b and c are continuously changed, then the total transformation process is known as a continuous wavelet transform. Meanwhile, the application cost and computational complexity are increased through continuous transformation. The discrete wavelet transform is computed and it is expressed as follows:

$$X_y(k, l) = \langle y(\tau), \vartheta_{k,l}(\tau) \rangle = \frac{1}{\sqrt{|b|}} \int_{\mathbb{R}} y_{\tau}(\tau) \overline{\Gamma\left(\frac{\tau - c}{b}\right)} d\tau \quad (18)$$

The variable k is utilized for determining the resolution at various scales for the multi-resolution features of wavelets. Two classes of the sub-signals and the original signal are computed and expressed as follows:

$$y(\tau) = b_0 + e_0 + e_{0-1} + \dots + e_1 \quad (19)$$

4.3. Embedded and Extracted Method of the Watermarking

The use of equilibrium optimization in the ROI selection process ensures that the optimal ROI is selected based on the degree of similarity between the host image and the watermarked image, which, in turn, improves the quality of the watermarking process. The use of fuzzy equilibrium optimization further enhances the accuracy and robustness of the watermark embedding and extraction processes by dynamically adjusting the parameters during the search process based on the degree of similarity between the host image and the watermarked image.

ROI Selection: Equilibrium optimization is used to select the region of interest (ROI) in the host image. The ROI is a set of pixels that will be used to embed the watermark. The equilibrium optimization algorithm searches for the optimal set of pixels to be used as the ROI, which maximizes the similarity between the original and watermarked images.

Watermark Generation: A binary watermark is generated based on the selected ROI. The watermark is a sequence of bits that will be embedded in the host image.

DWT Transformation: The watermark image is transformed into the time-frequency domain using discrete wavelet transform (DWT).

Sub-band Modification: The sub-bands of the DWT transformed watermark image are modified based on the magnitude of the wavelet coefficients to embed the watermark.

Singular Value Decomposition (SVD): SVD is applied to the modified sub-bands to obtain singular values that are used to embed the watermark further.

Watermarked Image: The modified sub-bands are combined to reconstruct the watermarked image.

Watermark Extraction

To extract the watermark from the watermarked image, the same ROI is selected using the equilibrium optimization algorithm. The ROI is used to extract the embedded watermark using a similar process as the embedding process.

Convert watermarked image to time domain: The watermarked image, which is in the frequency domain after the DWT process, is converted back to the time domain using inverse DWT.

Apply SVD: SVD is applied to each of the sub-bands of the watermarked image to obtain the singular values.

Compare singular values: The singular values of the watermarked image are compared with the singular values of the original watermark image to extract the watermark. The watermark is embedded in the sub-bands using the singular values of the original watermark image, which act as a secret key for watermark extraction.

Set a threshold: A threshold value is set to compare the singular values of the watermarked image and the original watermark image. If the difference between the singular values is less than the threshold, it is assumed that the watermark is present in the watermarked image.

Extract the watermark: The watermark is extracted by comparing the binary values of the watermark bits generated during the embedding process and the corresponding sub-bands of the watermarked image. If the value of the sub-band is greater than or equal to the threshold, the corresponding watermark bit is set to 1; otherwise, it is set to 0.

Reconstruct the watermark image: Finally, the extracted watermark bits are used to reconstruct the original watermark image.

5. Experimental Analysis and Discussions

The fuzzy equilibrium optimization (FEO) algorithm is proposed to provide secure, reliable and unbreakable watermarking for medical images. To improve the image quality, the medical image dataset was chosen, which contains MRI images, CT images and US images. Performance metrics such as embedding rate, embedding time, extraction time, number of pixels change rate, unified average changing intensity, coefficient index and entropy index are employed for performance evaluation. The remaining evaluation results are explained in the subsections below.

5.1. Experimental Setup

The performance of the proposed FEO algorithm is evaluated on MATLAB 2019b platform along with Intel Core i7 processor, 8 GB RAM and 2.2 GHz CPU.

5.2. Dataset Description

The medical image dataset used in this paper includes MRI images [24], CT images, and ultrasound (US) images [1]. In total, 70 medical images are selected and each image has a size of 512×512 as well as a watermark sized 64×64 .

5.3. Parameter Settings

To improve the performance of the proposed FEO algorithm, the optimal parameters are required, which are attained from the parameter tuning process. The achieved optimal parameter and its corresponding parameter values are explained in Table 1.

Table 1. Parameter settings.

Different Approaches	Optimal Parameters	Optimal Parameter Values
DWT	Number of epochs	100
	Number of neurons in the hidden layer	10
	Name of the optimizer	Adam
FEO	Variable probability	0.5
	Learning rate	0.8
	q_{best}	0.11
	H	5
	Arc rate	1.4
	Population size	50
	Number of iterations	100

5.4. Performance Evaluation Measures

A few performance evaluation measures are utilized for predicting the performance rate. The performance evaluation provides the equitable measurement and a high-level quality and quantity of the proposed work. The PSNR measures a quality of the original image and compressed image. The mathematical form of PSNR is given below,

$$PSNR = 10 \log_{10} \left(\frac{255^2}{MSE} \right) \quad (20)$$

$$MSE = \frac{1}{a} \sum_{j=1}^a (b_j - \hat{b}_j)^2 \quad (21)$$

where a , b_j and \hat{b}_j are denoted as number of samples, actual value and predicted value, respectively. Segmentation accuracy is the ratio of accurately segmented pixels to the total number of pixels and is calculated as,

$$\text{segmentation accuracy} = \frac{\text{number of correctly classified pixels}}{\text{total number of pixels}} \quad (22)$$

The correlation coefficient between the original and extracted watermark of NCC is presented in equation below,

$$\psi_{NCC} = \frac{\sum_{l=1}^{v_q \times v_s} v_l v'_l}{\sum_{l=1}^{v_q \times v_s} v_l^2 \sum_{l=1}^{v_q \times v_s} v'^2_l} \quad (23)$$

From the above equation, v_l and v'_l are represented as original watermark and extracted watermark, respectively. The pixel value changes are measured using UACI and NPCR, which are expressed follows:

$$\zeta_{UACI} = \frac{1}{AE} \left[\sum_{a,e}^{A,E} \frac{D_1(a,e) - D_2(a,e)}{H-1} \right] \times 100 \quad (24)$$

$$\zeta_{NPCR} = \frac{\sum_{a=1}^A \sum_{e=1}^E B(a,e)}{AE} \times 100 \quad (25)$$

where D_1 and D_2 depicts the encrypted images according to original image. a , e and $B(a, e)$ are the image width, image height and number of variations. The entropy index and coefficient index are the metrics to measure the performance of fuzzy model and are formulated as follows:

$$\text{entropy index} = \frac{-\sum_{l=1}^m \sum_{j=1}^n [W_{ji} \log W_{ji}]}{m} \quad (26)$$

$$\text{coefficient index} = \frac{\sum_{l=1}^m \sum_{j=1}^n W_{ji}^2}{m} \quad (27)$$

In our experiments, we added noise to the original medical images to test the robustness of our proposed algorithm against different types of noise. For each type of noise, we used specific noise generation techniques that are commonly used in the literature. For example, to add speckle noise to US images, we used the multiplicative speckle noise model, which adds noise to the image as follows:

$$I_{xy} = J_{xy} * N_{xy} \quad (28)$$

where I_{xy} is the noisy image, J_{xy} is the original image, and N_{xy} is a multiplicative noise term. The noise term is generated using gamma distribution with a shape parameter of 2 and a scale parameter of 0.5. Similarly, to add noise to the MRI and CT images, we used the Gaussian noise model, which adds noise to the image as follows:

$$I_{xy} = J_{xy} + N_{xy} \quad (29)$$

where I_{xy} is the noisy image, J_{xy} is the original image, and N_{xy} is an additive Gaussian noise term. The noise term is generated using a zero-mean Gaussian distribution with a standard deviation that is proportional to the noise level.

5.5. Performance Evaluation

The performance evaluation of the proposed FEO algorithm helps to identify the better performance of each metric. Table 2 illustrates the performance analysis to easily understand the performance of the current work.

Table 2. Overall performance evaluation.

Different Performance Metrics	Performance Rate
Peak signal to noise ratio	42.5 dB
Segmentation accuracy with respect to noise density	98.1%
Segmentation accuracy with respect to noise variance	98.3%
ζ_{NPCR}	0.985
ζ_{UACI}	0.3827
Embedding rate	0.021
Embedding time	3.2 s
Extraction time	2.1 s

5.6. Comparative Analysis

In this paper, different methods, namely the Lempel–Ziv–Welch-based lossless Compression Algorithm (LZW-LCA), zero watermarking algorithm (ZWA), chaotic integer wavelet transform-based least significant bit blind watermarking (CIWT-LSBBW) approach, firefly optimization algorithm (FOA) [25] and fuzzy equilibrium optimization (FEO) algorithm are utilized for attaining secure, reliable and unbreakable watermark images in the medical field. The PSNR analysis is performed by using different watermarking approaches such as LZW-LCA, ZWA, CIWT-LSBBW, FOA and the proposed FEO algorithm that is portrayed in Figure 3. The system robustness depends on the noise rate involved in the

system. The proposed FEO algorithm has a lower PSNR rate of 42.5 dB when compared with other existing methods. The remaining methods, LZW-LCA, ZWA, CIWT-LSBBW and FOA, have high PSNR rates of 69.8 dB, 58 dB, 65 dB and 51 dB, respectively. Table 3 shows the quality measurement of images for CT/MRI/US Images.

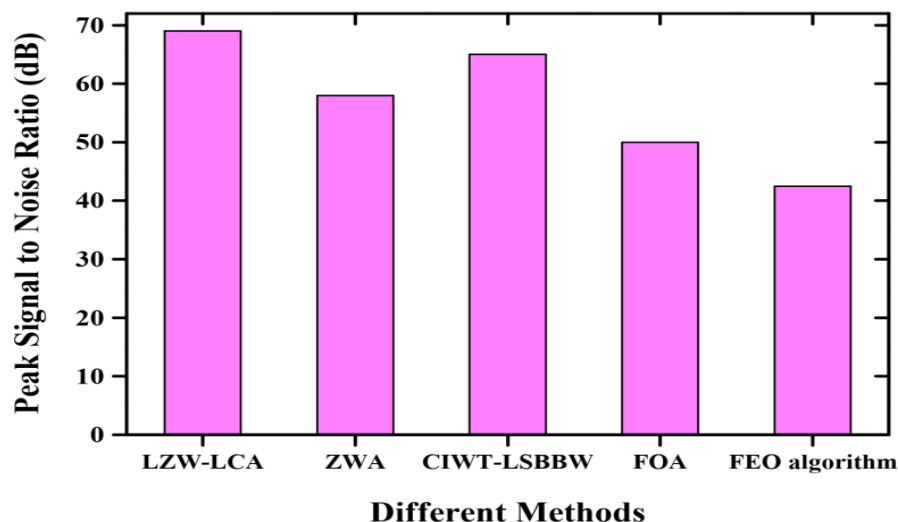


Figure 3. Comparative analysis of PSNR.

Figure 4 represents the segmentation accuracy of noise density with respect to various watermarking methods, such as CIWT-LSBBW, LZW-LCA, FOA, the proposed FEO algorithm and ZWA. In this experimental analysis graph, the proposed FEO algorithm achieved the highest accuracy of 98.1%, which denotes the robustness of the proposed watermarking system. The lowest segmentation accuracies of 64%, 89%, 55% and 79% are obtained from CIWT-LSBBW, LZW-LCA, FOA and ZWA. The segmentation accuracy of noise variance is depicted in Figure 5, which is evaluated according to the approaches of CIWT-LSBBW, LZW-LCA, ZWA, the proposed FEO algorithm and FOA. The maximum segmentation accuracy of 98.3% is predicted from the proposed FEO algorithm and other methods such as CIWT-LSBBW, LZW-LCA, ZWA and FOA, which provide minimum accuracies of 68%, 86%, 76% and 63%, respectively.

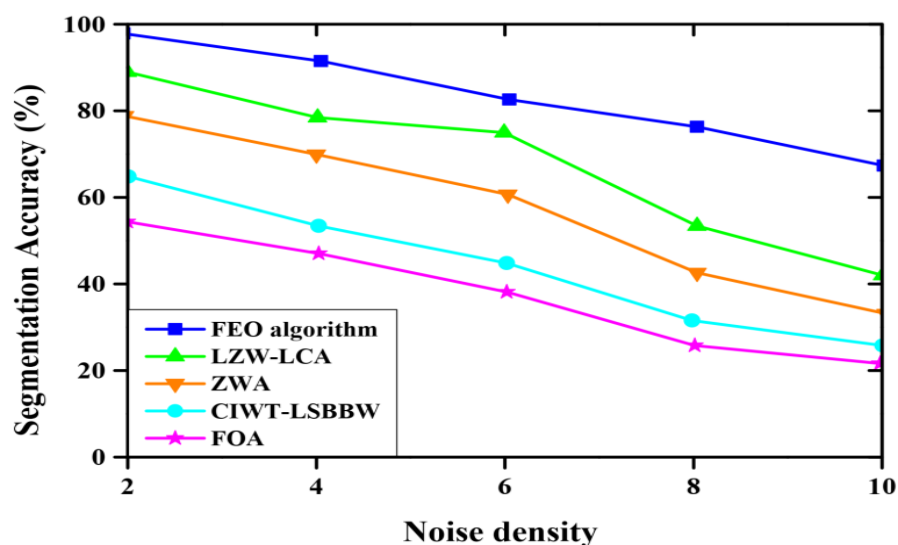
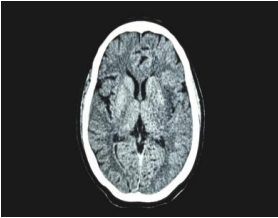
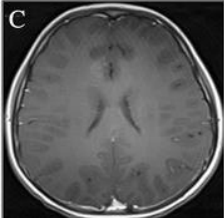
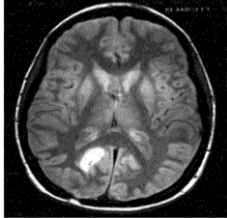
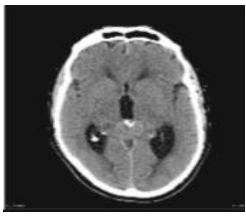




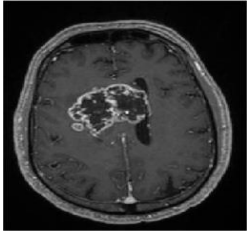
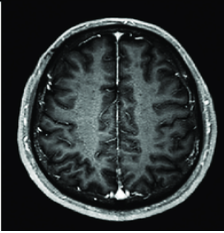
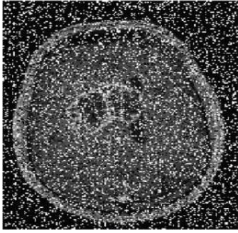
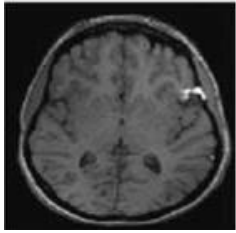
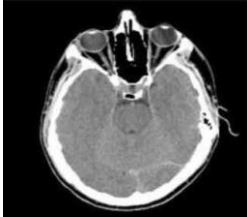

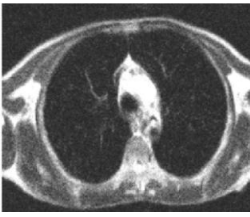





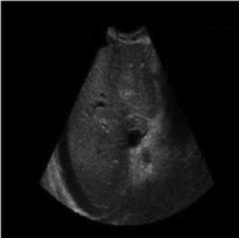


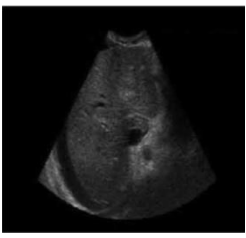


Figure 4. Comparative analysis of segmentation accuracy.

Table 3. Quality measurement of images for CT/MRI/US Images.

Types	Original Image	Embedded Image	Noise Image	Output
CT				
				
MRI				
				
US				
				

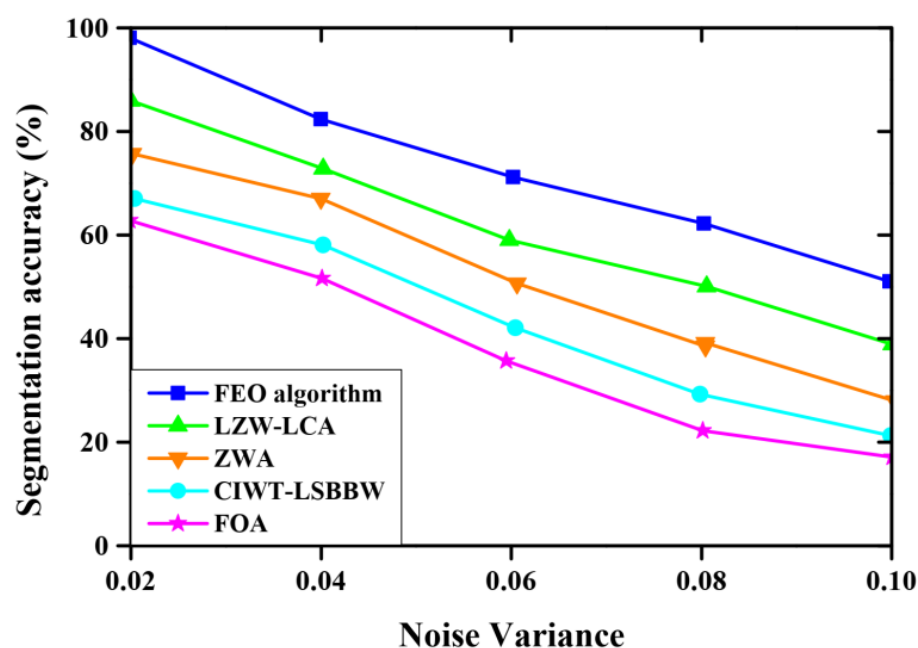


Figure 5. Segmentation accuracy of noise variance.

The comparative analysis of embedding rate, embedding time, extraction time, ζ_{NPCR} , ζ_{UACI} , coefficient index and entropy index are explained in Table 4. This table contains the performance rates and is computed using different methods, such as CIWT-LSBBW, LZW-LCA, FOA, the proposed FEO algorithm and ZWA. From this comparative analysis, the proposed FEO algorithm delineated a better performance: 0.021, 3.2 s, 2.1 s, 0.985, 0.3827, 0.979 and 0.0310 are achieved for the embedding rate, embedding time, extraction time, ζ_{NPCR} , ζ_{UACI} , coefficient index and entropy index.

Table 4. Comparison study.

Different Performance Metrics	Comparison Methods				
	CIWT-LSBBW	LZW-LCA	FOA	ZWA	Proposed FEO Algorithm
Embedding rate (bpp)	0.0018	0.0051	0.0097	0.0150	0.021
Embedding time (s)	5.2	4.9	6.3	4.5	3.2 s
Extraction time (s)	7	5.7	6.2	3.8	2.1 s
ζ_{NPCR}	0.904	0.956	0.897	0.962	0.985
ζ_{UACI}	0.258	0.3154	0.3381	0.2197	0.3827
Coefficient index	0.875	0.927	0.891	0.952	0.979
Entropy index	0.0789	0.0563	0.0617	0.0454	0.0310

6. Conclusions

The FEO algorithm is presented to provide a secure, reliable and unbreakable watermark image for medical images. To improve the image quality, the medical image dataset was chosen, which contains MRI images, CT image and US images. The performance metrics such as embedding rate, embedding time, extraction time, ζ_{NPCR} , ζ_{UACI} , coefficient index and entropy index are used to measure the performance rate. The different watermarking methods, namely the LZW-LCA, ZWA, CIWT-LSBBW approaches, FOA and the proposed FEO algorithm, were included in this paper for comparison study. The proposed medical image watermarking process achieved a PSNR rate of 42.5 dB, embedding time of 3.2 s and extraction time of 2.1 s. The proposed FEO algorithm displayed a better performance related to other existing methods. In the future, the robustness characteristics will be included in the proposed FEO algorithm to generate a semi-fragile digital watermarking scheme.

Author Contributions: Conceptualization, S.B. and A.A.; methodology, S.B. and A.A.; software, S.B.; validation, S.B. and A.A.; formal analysis, S.B. and A.A.; investigation, A.A.; resources, A.A.; data curation, S.B.; writing—original draft preparation, S.B.; writing—review and editing, A.A.; project administration, S.B. All authors have read and agreed to the published version of the manuscript.

Funding: The authors extend their appreciation to the Deputyship for Research and Innovation, Ministry of Education in Saudi Arabia, for funding this research work (Project number INST192).

Institutional Review Board Statement: Not Applicable.

Informed Consent Statement: Not Applicable.

Data Availability Statement: Not Applicable.

Conflicts of Interest: The authors declare no conflict of interest.

References

- Balasamy, K.; Suganyadevi, S. A fuzzy based ROI selection for encryption and watermarking in medical image using DWT and SVD. *Multimed. Tools Appl.* **2021**, *80*, 7167–7186.
- Sinhal, R.; Sharma, S.; Ansari, I.A.; Bajaj, V. Multipurpose medical image watermarking for effective security solutions. *Multimed. Tools Appl.* **2022**, *81*, 14045–14063. [\[CrossRef\]](#)
- Ravichandran, D.; Praveenkumar, P.; Rajagopalan, S.; Rayappan, J.B.B.; Amirtharajan, R. ROI-based medical image watermarking for accurate tamper detection, localisation and recovery. *Med. Biol. Eng. Comput.* **2021**, *59*, 1355–1372. [\[CrossRef\]](#) [\[PubMed\]](#)
- Dai, Z.; Lian, C.; He, Z.; Jiang, H.; Wang, Y. A novel hybrid reversible-zero watermarking scheme to protect medical image. *IEEE Access* **2022**, *10*, 58005–58016. [\[CrossRef\]](#)
- Borra, S.; Thanki, R. Crypto-watermarking scheme for tamper detection of medical images. *Comput. Methods Biomech. Biomed. Eng. Imaging Vis.* **2020**, *8*, 345–355. [\[CrossRef\]](#)
- Iwendi, C.; Jalil, Z.; Javed, A.R.; Reddy, T.; Kaluri, R.; Srivastava, G.; Jo, O. Keysplitwatermark: Zero watermarking algorithm for software protection against cyber-attacks. *IEEE Access* **2020**, *8*, 72650–72660. [\[CrossRef\]](#)
- Cedillo-Hernandez, M.; Cedillo-Hernandez, A.; Nakano-Miyatake, M.; Perez-Meana, H. Improving the management of medical imaging by using robust and secure dual watermarking. *Biomed. Signal Process. Control* **2020**, *56*, 101695. [\[CrossRef\]](#)
- Wang, W.; Xu, H.; Alazab, M.; Gadekallu, T.R.; Han, Z.; Su, C. Blockchain-based reliable and efficient certificateless signature for IIoT devices. *IEEE Trans. Ind. Inform.* **2021**, *18*, 7059–7067. [\[CrossRef\]](#)
- Alshanbari, H.S. Medical image watermarking for ownership & tamper detection. *Multimed. Tools Appl.* **2021**, *80*, 16549–16564.
- Thakur, S.; Singh, A.K.; Ghrera, S.P. NSCT domain-based secure multiple-watermarking technique through lightweight encryption for medical images. *Concurr. Comput. Pract. Exp.* **2021**, *33*, e5108. [\[CrossRef\]](#)
- Swaraja, K.; Meenakshi, K.; Kora, P. An optimized blind dual medical image watermarking framework for tamper localization and content authentication in secured telemedicine. *Biomed. Signal Process. Control* **2020**, *55*, 101665.
- Liu, X.; Lou, J.; Fang, H.; Chen, Y.; Ouyang, P.; Wang, Y.; Zou, B.; Wang, L. A novel robust reversible watermarking scheme for protecting authenticity and integrity of medical images. *IEEE Access* **2019**, *7*, 76580–76598. [\[CrossRef\]](#)
- Zeng, C.; Liu, J.; Li, J.; Cheng, J.; Zhou, J.; Nawaz, S.A.; Xiao, X.; Bhatti, U.A. Multi-watermarking algorithm for medical image based on KAZE-DCT. *J. Ambient. Intell. Humaniz. Comput.* **2022**, 1–9. [\[CrossRef\]](#)
- Patel, N.; Dwivedi, V.V.; Kothari, A. Hybrid Dct-Dwt Based Roi Medical Image Compression for Telemedicine Application. *Image* **2020**, *8*, 8. [\[CrossRef\]](#)
- Hu, K.; Wang, X.; Hu, J.; Wang, H.; Qin, H. A novel robust zero-watermarking algorithm for medical images. *Vis. Comput.* **2021**, *37*, 2841–2853. [\[CrossRef\]](#)
- Nazari, M.; Mehrabian, M. A novel chaotic IWT-LSB blind watermarking approach with flexible capacity for secure transmission of authenticated medical images. *Multimed. Tools Appl.* **2021**, *80*, 10615–10655. [\[CrossRef\]](#)
- Gong, C.; Li, J.; Bhatti, U.A.; Gong, M.; Ma, J.; Huang, M. Robust and secure zero-watermarking algorithm for medical images based on Harris-SURF-DCT and chaotic map. *Secur. Commun. Netw.* **2021**, *2021*, 3084153. [\[CrossRef\]](#)
- Dhall, S.; Gupta, S. Multilayered highly secure authentic watermarking mechanism for medical applications. *Multimed. Tools Appl.* **2021**, *80*, 18069–18105. [\[CrossRef\]](#)
- Song, Q.; Zhao, Q.; Wang, S.; Liu, Q.; Chen, X. Dynamic path planning for unmanned vehicles based on fuzzy logic and improved ant colony optimization. *IEEE Access* **2020**, *8*, 62107–62115. [\[CrossRef\]](#)
- Faramarzi, A.; Heidarinejad, M.; Stephens, B.; Mirjalili, S. Equilibrium optimizer: A novel optimization algorithm. *Knowl.-Based Syst.* **2020**, *191*, 105190. [\[CrossRef\]](#)
- Cheng, M.Y.; Prayogo, D. A novel fuzzy adaptive teaching–learning-based optimization (FATLBO) for solving structural optimization problems. *Eng. Comput.* **2017**, *33*, 55–69. [\[CrossRef\]](#)
- Rejeesh, M.R. Interest point based face recognition using adaptive neuro fuzzy inference system. *Multimed. Tools Appl.* **2019**, *78*, 22691–22710. [\[CrossRef\]](#)

23. Liu, Y.; Guan, L.; Hou, C.; Han, H.; Liu, Z.; Sun, Y.; Zheng, M. Wind power short-term prediction based on LSTM and discrete wavelet transform. *Appl. Sci.* **2019**, *9*, 1108. [[CrossRef](#)]
24. Clark, K.; Vendt, B.; Smith, K.; Freymann, J.; Kirby, J.; Koppel, P.; Moore, S.; Phillips, S.; Maffitt, D.; Pringle, M.; et al. The Cancer Imaging Archive (TCIA): Maintaining and Operating a Public Information Repository. *J. Digit. Imaging* **2013**, *26*, 1045–1057. [[CrossRef](#)] [[PubMed](#)]
25. Anand, A.; Singh, A.K. RDWT-SVD-firefly based dual watermarking technique for medical images (workshop paper). In Proceedings of the 2020 IEEE Sixth International Conference on Multimedia Big Data (BigMM), New Delhi, India, 24–26 September 2020; pp. 366–372.

Disclaimer/Publisher’s Note: The statements, opinions and data contained in all publications are solely those of the individual author(s) and contributor(s) and not of MDPI and/or the editor(s). MDPI and/or the editor(s) disclaim responsibility for any injury to people or property resulting from any ideas, methods, instructions or products referred to in the content.